

SCALAR MESONS FROM UNITARIZED CHIRAL PERTURBATION THEORY: N_c AND QUARK MASS DEPENDENCES

José R. Peláez and G. Ríos
Departamento de Física Teórica II. Facultad de CC. Físicas.
Universidad Complutense
28040 Madrid, SPAIN

Abstract

We review recent studies of light scalar meson properties by means of unitarization techniques, obtained from dispersion theory, and applied to the Chiral Perturbation Theory expansion. In particular, light scalars do not follow the N_c dependence of $\bar{q}q$ states although a subdominant $\bar{q}q$ component may be observed to arise for the $f_0(600)$ around 1 GeV, where another $\bar{q}q$ multiplet is believed to exist. Finally, we present our preliminary results on the quark mass dependence of the $f_0(600)$ and $\rho(770)$ resonances.

1 Introduction

Light hadron spectroscopy lies outside the applicability range of QCD perturbative calculations. Still, in this low energy region one can use Chiral Perturbation Theory (ChPT) [1] to obtain a model independent description of the dynamics of pions, kaons and etas. These particles are the Goldstone Bosons (GB) associated to the QCD spontaneous breaking of Chiral Symmetry and ChPT is built as a low energy expansion that contains those fields in the terms of a Lagrangian that respect all QCD symmetries, including its symmetry breaking pattern. The small quark masses of the three lightest flavors can be treated systematically within the perturbative chiral expansion and thus ChPT becomes a series in momenta and meson masses, generically $O(p^2/\Lambda^2)$. At lowest order there are no free parameters apart from masses and f_π , the pion decay constant, that sets the scale $\Lambda \equiv 4\pi f_\pi$. The chiral expansion can be renormalized order by order by absorbing the loop divergences in higher order counterterms, known as low energy constants (LEC), whose values depend on the specific QCD dynamics. That is, other theories

with spontaneous chiral symmetry breaking at the same scale will have the same leading order, but will differ in the values of the LEC.

The renormalized LEC have to be determined from experiment, since they cannot be calculated from perturbative QCD. However, thanks to the fact that ChPT has the same symmetries than QCD and that it should couple to different kind of currents in the same way, it is still possible to determine *in a model independent way* how the constants that appear in ChPT, and therefore the observables, depend on some QCD parameters. This is indeed the case of the leading dependence on the number of colors N_c and of the dependence on the quark masses.

2 Unitarization and dispersion theory

The unitarity of the S matrix implies that, for physical values of s , partial waves t^{IJ} of definite isospin I and angular momenta J for *elastic* meson-meson scattering should satisfy

$$\text{Im } t^{IJ} = \sigma |t^{IJ}|^2 \Rightarrow \text{Im } \frac{1}{t^{IJ}} = -\sigma \quad (1)$$

where $\sigma = 2p/\sqrt{s}$, and p is the CM momenta of the two mesons. Note that unitarity implies that $|t^{IJ}| \leq 1/\sigma$, and a strong interaction is characterized precisely by the saturation of this unitarity bound.

However, partial waves are obtained within ChPT as a low energy expansion $t \simeq t_2 + t_4 + t_6 + \dots$, (To simplify the notation, from now on we will drop the IJ indices.) where $t_{2k} \equiv O(p/(4\pi f_\pi))^{2k}$, and thus they cannot satisfy unitarity exactly, but just perturbatively, i.e:

$$\text{Im } t_2 = 0, \quad \text{Im } t_4 = \sigma t_2^2, \quad \text{etc...} \quad (2)$$

Unitarization methods extend the ChPT series to high energies by using the fact, remarked in eq.(1), that *the imaginary part of the inverse amplitude is known exactly*. Hence, we can approximate the real part of $\text{Re } t^{-1} \simeq t_2^{-2}(t_2 + \text{Re } t_4 + \dots)$ with ChPT, and find that

$$t \simeq = \frac{1}{\text{Re } t^{-1} - i\sigma} = \frac{t_2}{1 - t_4/t_2} \quad (3)$$

This is known as the one-channel Inverse Amplitude Method [2, 3]. A usual complaint is that the ChPT series is only valid at low energies, and there is no reason to use it beyond that regime.

However, not only the complete t , but also the *inverse amplitude* $1/t$ and the ChPT series to next to leading order (NLO) and beyond, have an

analytic structure with a “physical cut” extending from threshold to ∞ and a “left cut” from $-\infty$ up to the highest value of s allowed in the crossed channel ($s = 0$ if the two mesons are identical). It is then possible to write the following dispersion relation [3] for t_4

$$t_4 = b_0 + b_1 s + b_2 s^2 + \frac{s^3}{\pi} \int_{s_{th}}^{\infty} \frac{\text{Im } t_4(s') ds'}{s'^3 (s' - s - i\epsilon)} + LC(t_4). \quad (4)$$

where “LC” stands for a similar integral over the left cut and we have three subtractions to ensure convergence. A similar dispersion relation can be written for the function $G \equiv t_2^2/t$, by simply replacing t_4 by G and changing the name of the subtraction constants. Since t_2 is real, these two functions have opposite imaginary parts on the physical cut so that their contributions from the “physical cut” integral are *exactly* opposite. Their subtraction constants correspond to the value of these functions at $s = 0$ where it is perfectly justified to use the ChPT expansion. And finally, their contributions from the left cut are also opposite from each other, but this time only up to the NNLO ChPT terms. This guarantees a good description of the integrand only at low energies, but that is precisely the region that has been weighted by the three subtractions.

Therefore, note that the IAM is actually exact on the physical region and only uses the ChPT approximations for the subtraction constants at $s = 0$, where the use of ChPT is totally justified, and for the left cut, where the use of ChPT might not be justified at large $|s'|$, but the influence of this region is dumped by the subtractions. The use of the IAM is even more justified if used sufficiently far from this left cut, since this has an additional $(s - s')$ suppression. In summary, there are no model dependencies in the approach, but just approximations to a given order in ChPT, and indeed the IAM can be derived not only at NLO but also at NNLO.

Remarkably, the simple formula of the IAM, eq.(3), is able to describe the $\pi\pi$ and πK scattering data not only at low energies, where it reproduces the ChPT series, but also in the resonance region. This is done with values of the ChPT parameters that are compatible with the values obtained within standard ChPT.

In addition, the IAM generates the poles [3,4] associated to the resonances in the second Riemann sheet. This is of relevance since, in particular, the scalar resonances are the subject of intense debate that has been lasting for several decades, and as we have seen, the IAM is able to generate their poles from first principles like unitarity, analyticity and the QCD chiral symmetry breaking, without introducing these resonances by hand. Thus, we can study, without any a priori assumption, the nature of these states as follows from first principles and QCD.

3 N_c behavior

The QCD $1/N_c$ expansion [5] allows for a clear identification of a $\bar{q}q$ resonance, since it becomes a bound state, whose width follows an $O(1/N_c)$ behavior, whereas its mass should behave as $O(1)$. For our purposes, the relevant observation is that the leading $1/N_c$ behavior of the ChPT constants is known in a model independent way. Thus, in order to know the leading N_c behavior of the resonances generated with the IAM, we just have to change the ChPT parameters according to their established N_c scaling properties. For instance, the pion decay constant scales as $O(\sqrt{N_c})$, and we thus substitute f_π by $f_\pi\sqrt{N_c}/3$. Similar replacements, but according to their respective N_c scaling, have to be done with all ChPT parameters.

This procedure [4, 6] was first applied to the coupled channel IAM [4, 7] using the one loop SU(3) ChPT amplitudes, that also include kaons and etas, and the result was that the light vector resonances $\rho(770)$ and $K^*(982)$ followed remarkably well the expected behavior of $\bar{q}q$ states. In contrast, the members of the light scalar nonet, namely, the sigma or $f_0(600)$, the kappa or $K_0(800)$, as well as the $f_0(980)$ and $a_0(980)$ resonances, all showed a behavior at odds with that of $\bar{q}q$ states (Only the $a_0(980)$ could display a $\bar{q}q$ behavior in a limited corner of parameter space). It follows that *the dominant component of light scalar mesons does not have a $\bar{q}q$ nature*.

Very recently [8] we have extended the analysis to two loops in SU(2) ChPT, using the IAM one-channel formalism just described above to NNLO. In addition, we have developed a quantitative measure of how close a resonance is to a $\bar{q}q$ behavior: Taking into account subleading orders, to consider a resonance a $\bar{q}q$ state, it is enough that

$$M_{N_c}^{\bar{q}q} = \widetilde{M} \left(1 + \frac{\epsilon_M}{N_c} \right), \quad \Gamma_{N_c}^{\bar{q}q} = \frac{\widetilde{\Gamma}}{N_c} \left(1 + \frac{\epsilon_\Gamma}{N_c} \right), \quad (5)$$

where \widetilde{M} and $\widetilde{\Gamma}$ are unknown but N_c independent and the subleading terms have been gathered in $\epsilon_M, \epsilon_\Gamma \simeq 1$, since we expect *generically* 30% uncertainties at $N_c = 3$. Thus, for a $\bar{q}q$ state, the *expected* M_{N_c} and Γ_{N_c} can be obtained from those at $N_c - 1$ generated by the IAM, as follows

$$M_{N_c}^{\bar{q}q} \simeq M_{N_c-1} \left[1 + \epsilon_M \left(\frac{1}{N_c} - \frac{1}{N_c-1} \right) \right] \equiv M_{N_c-1} + \Delta M_{N_c}^{\bar{q}q}, \quad (6)$$

$$\Gamma_{N_c}^{\bar{q}q} \simeq \frac{\Gamma_{N_c-1}(N_c-1)}{N_c} \left[1 + \epsilon_\Gamma \left(\frac{1}{N_c} - \frac{1}{N_c-1} \right) \right] \equiv \frac{\Gamma_{N_c-1}(N_c-1)}{N_c} + \Delta \Gamma_{N_c}^{\bar{q}q}.$$

Note the $\bar{q}q$ index for quantities obtained *assuming* a $\bar{q}q$ behavior. The reason to write the N_c values from those at $N_c - 1$ is to be able to calculate from

what N_c a resonance starts behaving as a $\bar{q}q$, which is of interest to search for subdominant $\bar{q}q$ components. Thus, we can define an *averaged* $\bar{\chi}_{\bar{q}q}^2$ to check how close a resonance is to a $\bar{q}q$ behavior, as follows:

$$\bar{\chi}_{\bar{q}q}^2 = \frac{1}{2n} \sum_{N_c=4}^n \left[\left(\frac{M_{N_c}^{\bar{q}q} - M_{N_c}}{\Delta M_{N_c}^{\bar{q}q}} \right)^2 + \left(\frac{\Gamma_{N_c}^{\bar{q}q} - \Gamma_{N_c}}{\Delta \Gamma_{N_c}^{\bar{q}q}} \right)^2 \right] \quad (7)$$

When this quantity is smaller than one, it indicates a $\bar{q}q$ behavior, whereas a larger value indicates that it does not behave predominantly as such. Note also that imposing the minimization of the $\bar{\chi}^2$ in eq.(7) we could try to force a given $\bar{q}q$ behavior for a given resonance when fitting data.

When evaluating eq.(7) above, one has to be careful not to consider too large N_c values. The reason is that, after all, we are interested in the physical state at $N_c = 3$ and, most likely, states are a mixture of different components with different N_c behavior. By allowing for too large values of N_c we could be altering too radically the nature of the state, and, since $\bar{q}q$ states are expected to survive in the large N_c limit, whereas other kind of states, like tetraquarks, glueballs, etc... do not, even insignificant admixtures of $\bar{q}q$ at $N_c = 3$ could become dominant for sufficiently large N_c . Thus, the most relevant information will come from N_c not too far from $N_c = 3$ and we consider N_c values smaller than one order of magnitude its physical value of 3, let us say $N_c < 20$.

In this respect, J.A. Oller raised an interesting concern at the end of my talk in this conference, about the absence of $\eta'(980)$ in our calculations. Certainly, the η' mass is due to the $U_A(1)$ anomaly, and decreases like $1/\sqrt{N_c}$. If we were to consider very large N_c , this particle should be definitely included in our calculations, because it would become the most relevant degree of freedom of QCD at very large N_c . However, if we limit ourselves to, say $N_c = 20$, its mass would be $950 \text{ MeV} \times \sqrt{3/20} \simeq 370 \text{ MeV}$, so, it is still much heavier than the pions that can still be considered as the only low energy degrees of freedom of the theory (Furthermore, its contribution would be similar to that of kaon loops, although there are both neutral and charged kaon loops, whereas we only have one η'). This is an additional reason why it would be just wrong to consider too large values of N_c to draw conclusions about the nature of the sigma.

Therefore, with the measure in eq.(7) and $n = 20$, we are able to quantify the deviation of the $f_0(600)$ from the $\bar{q}q$ behavior: at NLO, even in the most favorable case when we try to impose that it behaves as a $\bar{q}q$, the data fit yields a $\bar{\chi}_{\bar{q}q}^2 = 125$ for the $f_0(600)$.

When using the NNLO (two loop ChPT calculation), we have many more ChPT parameters, which are not well known, and give a great deal of free-

dom. For the NNLO low energy constants (LECS) we thus use standard estimates [9] with a 100% uncertainty. Still, there are large correlations and some very weak dependences on some of these parameters that can be driven far from their standard values for negligible improvements in the χ^2 of the data fit. For that reason we stabilize the values of the LECS, imposing also the minimization of a χ_{LECS}^2 together with that of the data. Also, using eq.(7), we impose the $\rho(770)$, which is a well established $\bar{q}q$ state, to behave as such. Thus, at two loops, we find that the $f_0(600)$ comes out with $\bar{\chi}_{\bar{q}q}^2 = 4$ in the most favorable case when we try to impose it to behave as a $\bar{q}q$. Even relaxing the ρ $\bar{q}q$ behavior, we still get $\bar{\chi}_{\bar{q}q}^2 = 3.5$ for the $f_0(600)$. In conclusion, *the two loop IAM confirms once again that the $f_0(600)$ does not behave predominantly as a $\bar{q}q$ state*, whereas that behavior is nicely followed by the ρ , whose $\bar{\chi}_{\bar{q}q}^2 < 0.35$ at NLO and $\bar{\chi}_{\bar{q}q}^2 = 0.93$ at NNLO.

We show in Fig.1 the NNLO behavior of the ρ and $f_0(600)$ mass and width. In the top figure, we show the $N_c = 3$ behavior of the ρ . The full dots represent the values, for different N_c , of its "pole mass", M , whereas the empty dots represent its "pole width", Γ , both normalized to their physical values at $N_c = 3$. It can be clearly seen that, already for very low N_c , M/M_3 starts behaving as $O(1)$ and Γ/Γ_3 as $O(1/N_c)$, as expected for a $\bar{q}q$ state. As commented above, the behavior shown in this plot yields $\bar{\chi}_{\bar{q}q}^2 = 0.93$ for the ρ . In contrast, in the bottom figure, and with the same conventions, we show the N_c behavior of the σ or $f_0(600)$. This time we are also imposing in the fit minimization that it should behave as a $\bar{q}q$ state. Obviously it does not, at least until $N_c \simeq 8$, and its $\bar{\chi}_{\bar{q}q}^2 = 4$. Despite the σ is still not behaving predominantly as a $\bar{q}q$ state, the price due to trying to impose such behavior is that the fit suffers a clear deterioration, since the data now has a $\chi^2/dof = 1.5$ (compared to 1.1 before) and the ρ now has $\bar{\chi}_{\bar{q}q}^2 = 1.3$, thus with a much worse $\bar{q}q$ behavior.

Remarkably, it is also clear that the σ or $f_0(600)$ follows a $\bar{q}q$ behavior for $N_c > 8$ or 10. This suggests the existence of a *subdominant* $\bar{q}q$ behavior in the σ or $f_0(600)$ that originates at a mass around twice that of the sigma $\simeq 1\text{GeV}$, where a $\bar{q}q$ nonet is usually located.

4 Quark mass dependence

We now present our very preliminary work [10] on the quark mass dependence of the mass and widths of the σ and ρ mesons, which could be of interest to compare with lattice studies, where the small physical masses of light quarks are hard to implement.

With the IAM we can also study the quark mass dependence of the light

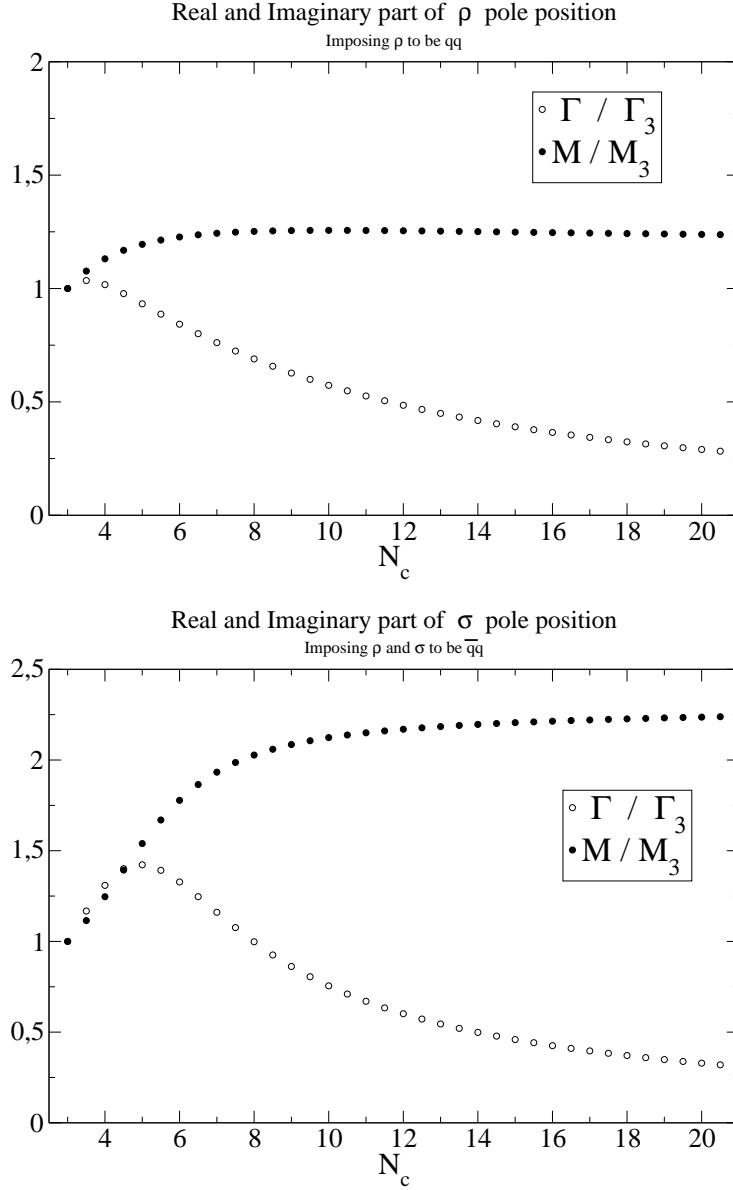


Figure 1: Mass and width dependence on N_c for the ρ (Top) and σ (Bottom) resonances. We have normalized all M and Γ to their respective physical values at $N_c = 3$. Note that, already for N_c close to 3, the ρ mass and width follow nicely the respective $O(1)$ and $O(1/N_c)$ behavior expected for a $\bar{q}q$ state. In contrast, the σ does not behave predominantly as such, but only develops, above $N_c = 8$ or 10, a *subdominant* $\bar{q}q$ behavior with a mass $\simeq 1$ GeV.

resonances by changing the meson masses in the amplitudes, which is equivalent to change quark masses, since, to leading order $M_\pi^2 \sim m_q + \dots$. We have done this in $SU(2)$ Unitarized ChPT at NLO. In $\pi\pi$ scattering at NLO there appear four LECs l_1, \dots, l_4 . Phase shifts are almost insensitive to l_3^r and l_4^r , for which we take the values in [1]: $l_3^r = 0.8 \pm 3.8$, $l_4^r = 6.2 \pm 5.7$, evaluated at a renormalization scale of $\mu = 770$ MeV. In contrast, we make a data fit for l_1^r and l_2^r , finding $l_1^r = -3.7 \pm 0.2$, $l_2^r = 5.0 \pm 0.4$, in fairly good agreement with standard values. Finally, when changing pion masses we have to take into account that amplitudes are customarily written [1] in terms of the μ independent LECs \bar{l} [1] and the physical pion decay constant $f_\pi = f_0 \left(1 + \frac{M_\pi^2}{16\pi^2 f_0^2} \bar{l}_4 + \dots\right)$ that depend explicitly on the pion mass.

We have taken two criteria to set the applicability limit of our method, that is, the maximum value of the pion mass we can use. First, we do not want to spoil the chiral expansion, and second, we do not want the two-pion threshold to reach the $K\bar{K}$ threshold. Taking into account that $SU(3)$ ChPT works well with a kaon mass of ~ 495 MeV, and that, according to NLO ChPT, if we set $M_\pi \simeq 500$ MeV the kaon mass becomes ~ 600 MeV, this means that for 500 MeV pions, $\pi\pi$ scattering is still elastic for about 200 MeV above threshold. Hence the above criteria impose an applicability bound of $M_\pi \simeq 500$ MeV. To go beyond that we would need a coupled channel $SU(3)$ formalism.

We show in Fig.2 how the ρ and $f_0(600)$ poles in the second Riemann sheet move as M_π changes. Both the ρ and σ mass increase with the pion mass, but that of the σ grows faster. In addition, both widths decrease, partly due to phase space reduction (the two-pion threshold grows faster than both resonance masses). When the two-pion threshold reaches the σ mass, its pole remains for a short while on the second sheet with a non-zero width but quickly reaches the real axis where it meets its conjugate partner from the upper plane and splits again into two poles corresponding to virtual bound states located on the real axis below threshold. As the pion mass keeps increasing, one of those "virtual state" poles moves toward threshold and jumps into the first sheet, whereas the other one remains in the second sheet. Although, of course, this happens for very large M_π masses, such an analytic structure, with two very asymmetric poles in different sheets of an angular momentum zero partial wave, may be a signal of molecular structure, as discussed by M. Pennington in this conference.

Finally, as the pion mass increases, the ρ pole moves toward the real axis and just when threshold reaches its mass it jumps into the real axis on the first sheet, thus becoming a traditional bound state, while its conjugate partner remains on the second sheet practically at the very same position as

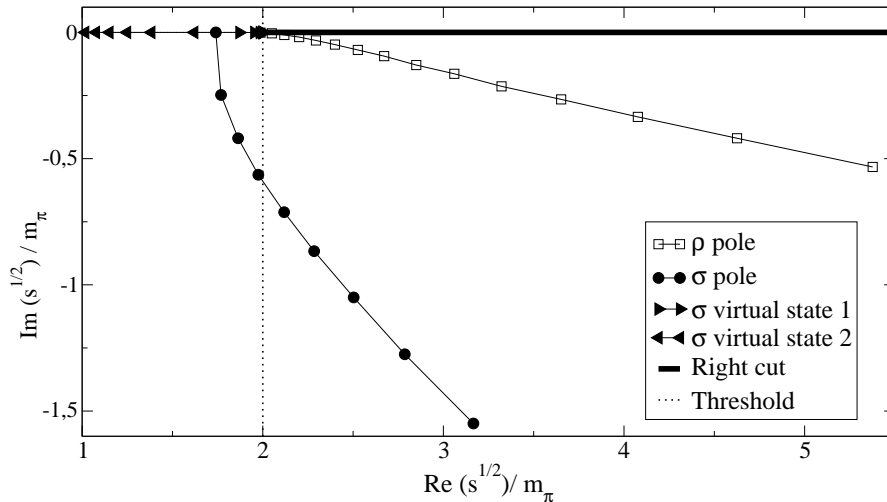


Figure 2: ρ and σ complex plane pole movement with increasing pion mass. To ease the comparison of the pole position relative to the two-pion threshold we normalize by the pion mass that is changing. Note how the sigma pole moves toward the real axis below threshold where it splits in two virtual states, whereas the ρ pole just moves toward threshold.

the one in the first.

A publication with further details is in preparation [10] including results of the $f_0(600)$ and $\rho(770)$ mass and width evolution with the pion mass as well as a comparison with other works and lattice results. Estimates of uncertainties and possibly an extension to the SU(3) coupled channel case are presently in progress.

Acknowledgments

J.R. Peláez thanks the MENU07 organizers for their kind invitation and the great scientific organization. We also thank J.A. Oller and C. Hanhart for useful discussions and comments.

Research partially funded by Spanish CICYT contracts FPA2005-02327, BFM2003-00856 as well as Banco Santander/Complutense contract PR27/05-13955-BSCH, and part of the EU integrated infrastructure initiative HADRON-PHYSICS PROJECT, under contract RII3-CT-2004-506078.

References

- [1] S. Weinberg, *Physica* **A96** (1979) 327. J. Gasser and H. Leutwyler, *Annals Phys.* **158** (1984) 142; *Nucl. Phys. B* **250** (1985) 465.
- [2] T. N. Truong, *Phys. Rev. Lett.* **61** (1988) 2526. *Phys. Rev. Lett.* **67**, (1991) 2260; A. Dobado, M.J.Herrero and T.N. Truong, *Phys. Lett.* **B235** (1990) 134.
- [3] A. Dobado and J. R. Pelaez, *Phys. Rev. D* **47** (1993) 4883. *Phys. Rev. D* **56** (1997) 3057.
- [4] J. R. Pelaez, *Mod. Phys. Lett. A* **19**, 2879 (2004)
- [5] G. 't Hooft, *Nucl. Phys. B* **72** (1974) 461. E. Witten, *Annals Phys.* **128** (1980) 363.
- [6] J. R. Pelaez, *Phys. Rev. Lett.* **92**, 102001 (2004)
- [7] F. Guerrero and J. A. Oller, *Nucl. Phys. B* **537** (1999) 459 [Erratum-ibid. *B* **602** (2001) 641]. A. Gómez Nicola and J. R. Peláez, *Phys. Rev. D* **65** (2002) 054009 and *AIP Conf. Proc.* **660** (2003) 102 [hep-ph/0301049].
- [8] J. R. Pelaez and G. Rios, *Phys. Rev. Lett.* **97**, 242002 (2006)
- [9] J. Bijnens *et al.*, *Nucl. Phys. B* **508**, 263 (1997)
- [10] C. Hanhart, J.R. Peláez and G. Ríos, *in preparation*.